A-priori and a-posteriori assessment of LES subgrid models for liquid jet atomization

Sebastian Ketterl & Markus Klein

Department of Aerospace Engineering
Universität der Bundeswehr München
Werner-Heisenberg Weg 39, 85577 Neubiberg, Germany
sebastian.ketterl@unibw.de

ABSTRACT

This contribution is targeted towards large eddy simulation (LES) of turbulent two-phase flow. A variety of LES models for the subgrid stress tensor and the additional unclosed subgrid scale (SGS) terms which emerge due to filtering across the discontinuous phase interface are first a-priori assessed with respect to explicitly filtered direct numerical simulation (DNS) data of liquid jet atomization. Afterwards, a-posteriori LES including the investigated SGS models are conducted and compared to DNS results by means of flow statistics and droplet size distributions. The influence of eddy viscosity models remains small. It is observed that they tend to dampen the disintegration of the jet. It is shown that the primary breakup strongly depends on the numerical discretization of the nonlinear momentum advection term. A-priori and a-posteriori studies demonstrate that the numerical error has the same order of magnitude and to some extend dominates the effect of the subgrid stress model. Incorporating the unresolved surface tension force and the subgrid interfacial term ameliorates a-posteriori LES results. Subgrid capillary forces enhance the disintegration while the subgrid interfacial term lead to later ligament breakup.

INTRODUCTION

The atomization of liquids describes the disintegration of a liquid core into a large number of droplets. DNS of liquid jet atomization for industrial applications, e.g. fuel injection in combustion devices, will remain out of scope in the near future due the excessive computational costs stemming from a large range of length and time scales. In order to predict the primary breakup, it is strived for an LES framework for turbulent two-phase flow systems and the required development of appropriate SGS models is one of the urgest challenges (Tryggvason et al., 2013). However, LES for two-phase flows including the transport of an interface remains as of this day a largely unexplored area. Developments towards LES of atomization are difficult because the breakup of turbulent liquid jets itself is still not fully understood. Despite its technical relevance, profound knowledge about turbulence-interface interaction in the context of LES leading to the formation of droplets is rare.

In turbulent two-phase LES large scales of turbulence and the large deformations of the interface are explicitly described. In contrast to single phase flow, not only turbulent but also interfacial structures remain smaller than the mesh size. The effects of the smallest turbulent eddies, unresolved interface dynamics and their interaction with the resolved large scales must be incorporated in the LES framework. This subgrid scale turbulence-interface interaction is captured by additional terms in the governing LES equations which appear due to the filtering of variables across the discontinuous phase interface. These unclosed terms cannot be computed directly and must be treated through appropriate modeling. It has been shown in a-priori DNS studies that these subgrid contributions are in general not negligible (Labourasse et al., 2007; Chesnel et al., 2011*a*).

Modeling complexity arises since turbulence is generated or modulated by the presence of the interface and volume fraction fluctuations (Vincent et al., 2008). Most subgrid models however are based on the assumption that subgrid fluctuations only originate from turbulence or that gradients originate only from large-scale turbulence (Chesnel et al., 2011*b*). In Ketterl and Klein (2017), a variety of subgrid models known from single phase flow or combustion have been adapted and applied to two-phase flows, as well as new models have been proposed. These models were a-priori assessed with respect to explicitly filtered DNS data of jet atomization but no a-posteriori LES has been presented so far. The goal of this work is to extend a-priori studies with a-posteriori LES computations and statistical a-posteriori SGS model evaluations.

Most a-posteriori LES of primary spray formation neglect the subgrid contributions stemming from the presence of the interface (De Villiers et al., 2004). Only the subgrid scale stress tensor arising from the nonlinear momentum advection term known from single phase flow is modelled. A posteriori LES results obtained with this approach reveal a strong mesh dependence on liquid breakup since the interaction of turbulence with the interface in the shear layer between the phases is not accounted for. Only large scale instabilities contribute to the jet breakup. Recent studies by Chesnel et al. (2011*b*) underline the potential of improving results when the interfacial subgrid term $\tau_{\alpha u,i}$ (see Eqn. (12)) is taken into account in a-posteriori LES calculations or if subfilter capillary forces $\tau_{\alpha u,i}$ (see Eqn. (11)) are included (Herrmann, 2013).

DNS AND LES METHODOLOGY

Low Mach-number primary atomization can be described by the one-fluid formulation of the incompressible Navier-Stokes equations in non-conservative form

$$\frac{\partial u_i}{\partial x_i} = 0 \tag{1}$$

$$\rho\left(\frac{\partial u_i}{\partial t} + \frac{\partial u_i u_j}{\partial x_j}\right) = -\frac{\partial p}{\partial x_i} + \frac{\partial}{\partial x_j}\left(\mu\left(\frac{\partial u_i}{\partial x_j} + \frac{\partial u_j}{\partial x_i}\right)\right) + \sigma n_i \kappa \delta_S \tag{2}$$

where ρ and μ denote the fluid density and viscosity, u_i and p are the velocity components and the pressure. The curvature is described by κ, σ denotes the constant surface tension and the normal vector on the surface is represented by n_i. The Dirac distribution δ_S restricts the presence of the surface tension term to the vicinity of the interface. The volume fraction α implicitly defines the interface between the two immiscible fluids. The sharp interface is tracked by the advection equation

$$\frac{\partial \alpha}{\partial t} + \frac{\partial}{\partial x_i}(\alpha u_i) = 0. \tag{3}$$

while the volume fraction equals one in the liquid phase.

Computations are performed with the free code *PARIS* (Arrufat et al., 2017). Numerical schemes are implemented as described in Tryggvason et al. (2011) where further details on numerical methods and references can be found. The incompressible Navier-Stokes equations with sharp interfaces Eqns. (1)-(3) are solved by a projection method including a second-order predictor-corrector time-stepping method. The equations are discretized by a finite-volume approach using a regular, cubic staggered grid. The viscous terms are treated explicitly by a second-order central difference scheme. A third-order QUICK and WENO, or second-order central difference (CDS) scheme discretize the advection term. Local interface curvatures are calculated by the height-function method. A balanced Continuous-Surface-Force method computes the surface tension force. The elliptic pressure equation is solved by a BiCGSTAB solver. The interface is advected by a Volume-of-Fluid (VOF) method realized by a Lagrangian-Explicit advection step and a Mixed Youngs-Centered interface reconstruction. Near the interface, momentum advection is conducted in a consistent manner with the VOF advection. These numerical schemes are used for DNS and LES computations. Within this framework, the original DNS solver is extended towards a two-phase LES code.

The DNS solves the governing equations while resolving the full range of lengths scales down to the Kolmogorov scale and while capturing interfacial structures down to the thinnest ligaments and smallest droplets. LES in contrast introduces a separation of scales. Large scale flow properties are accounted for and explicitly described while scales smaller than a certain cut off length are not captured and need to be modeled. The scale separation is carried out by a spatial low-pass filter operation

$$\bar{\phi}(x) = G * \phi(x) = \int \phi(y)\, G(x-y,x)\, \mathrm{d}y \tag{4}$$

which corresponds to a convolution with a filter function G. The overbar $\bar{\phi}$ denotes resolved flow field variables. Applying the filter kernel to the conservation equations in conservative form yields the governing LES equations. The filtered Navier-Stokes equations and filtered volume fraction advection equation (Labourasse et al., 2007) in conservative form read:

$$\frac{\partial \overline{u}_i}{\partial x_i} = 0 \tag{5}$$

$$\begin{aligned}\frac{\partial \overline{\rho}\,\overline{u}_i}{\partial t} + \frac{\partial \overline{\rho}\,\overline{u}_i\overline{u}_j}{\partial x_j} &= -\frac{\partial \overline{p}}{\partial x_i} + \frac{\partial}{\partial x_j}\left(\overline{\mu}\left(\frac{\partial \overline{u}_i}{\partial x_j} + \frac{\partial \overline{u}_j}{\partial x_i}\right)\right) + \overline{\sigma}\,\overline{n}_i\,\overline{\kappa}\,\overline{\delta}_S \\ &\quad - \frac{\partial\, \tau_{uu,ij}}{\partial x_j} - \frac{\partial\, \tau_{tt,i}}{\partial t} + \frac{\partial\, \tau_{\mu S,ij}}{\partial x_j} + \tau_{nn,i}\end{aligned} \tag{6}$$

$$\frac{\partial \overline{\alpha}}{\partial t} + \frac{\partial}{\partial x_i}(\overline{\alpha}\,\overline{u}_i) = -\frac{\partial}{\partial x_i}\tau_{\alpha u,i}. \tag{7}$$

Due to the filtering across the phase interface, the following unclosed subgrid contributions emerge:

$$\tau_{\rho uu,ij} = \overline{\rho\, u_i u_j} - \overline{\rho}\,\overline{u_i}\,\overline{u_j} \tag{8}$$

$$\tau_{tt,i} = \overline{\rho\, u_i} - \overline{\rho}\,\overline{u_i} \tag{9}$$

$$\tau_{\mu S,ij} = \overline{\mu\,(\frac{\partial u_i}{\partial x_j} + \frac{\partial u_j}{\partial x_i})} - \overline{\mu}\,(\frac{\partial \overline{u}_i}{\partial x_j} + \frac{\partial \overline{u}_j}{\partial x_i}) \tag{10}$$

$$\tau_{nn,i} = \overline{\sigma\, n_i\, \kappa\, \delta_S} - \overline{\sigma}\,\overline{n_i}\,\overline{\kappa}\,\overline{\delta_S} \tag{11}$$

$$\tau_{\alpha u,i} = \overline{\alpha\, u_i} - \overline{\alpha}\,\overline{u_i} \tag{12}$$

These terms contain the subgrid scale turbulence-interface interaction. The effect of the smallest scales of turbulent and interfacial motion which are not resolved by the LES mesh must be incorporated through modeling. The tensor $\tau_{\mu S,ij}$ is denoted as diffusive term, the unresolved surface tension force is represented by $\tau_{nn,i}$, the tensor $\tau_{tt,i}$ is the temporal term and $\tau_{\alpha u,i}$ the interfacial term. The SGS stress tensor $\tau_{uu,ij}$ arises from filtering the nonlinear term and is known from single phase flow. Togehter with the temporal term $\tau_{tt,i}$, this is the dominating subgrid term in the momentum equation (Toutant et al., 2008; Liovic and Lakehal, 2007; Ketterl and Klein, 2017) and numerous closure models have been developed. A selection of promising models is presented next.

Eddy viscosity type models relate turbulent transport to molecular transport through an additional viscosity based on Boussinesq's hypotheses

$$\tau_{uu,ij} = -2\,\nu_t\,\overline{S}_{ij} \tag{13}$$

where ν_t is the kinematic turbulent eddy viscosity and $S_{ij} = (\partial_i u_j + \partial_j u_i)/2$ denotes the deformation tensor. The static Smagorinsky model, written as SSM-C where the index C denotes the convective SGS term, specifies the eddy viscosity depending on the shear rate as

$$\nu_t^{SSM-C} = (C_s\Delta)^2\,\left|\overline{S}_{ij}\right|,\ \left|\overline{S}_{ij}\right| = \sqrt{2\,\overline{S}_{ij}\overline{S}_{ij}}. \tag{14}$$

The parameter $C_s = 0.18$ is set constant. The Nicoud et al. (2011) sigma model (SσM-C) reads

$$\begin{aligned}\nu_t^{S\sigma M-C} &= (C_\sigma\Delta)^2\,\frac{\sigma_3\,(\sigma_1-\sigma_2)(\sigma_2-\sigma_3)}{\sigma_1^2} \\ G_{ij} &= \frac{\partial \overline{u}_i}{\partial x_j}\frac{\partial \overline{u}_j}{\partial x_i},\ \ \sigma_1 \geq \sigma_2 \geq \sigma_3 = \sqrt{\mathrm{Eig}(G_{ij})}\end{aligned} \tag{15}$$

and has the property to vanish as soon as the resolved field is either two-dimensional or two-component. The closure is able to represent the appropriate cubic behavior of the turbulent viscosity in the vicinity of solid boundaries which seems to be promising regarding the analogy of the wall-turbulence and interface-turbulence interaction (Fulgosi et al., 2003). Vreman's model (V-C) (Vreman, 2004) is designed for the use in turbulent shear flows and states

$$\begin{aligned}\nu_t^{V-C} &= C_V\sqrt{\frac{B_\beta}{\alpha_{ij}\alpha_{ij}}},\ \ \alpha_{ij} = \frac{\partial\, \overline{u}_j}{\partial\, x_i},\ \ \beta_{ij} = \Delta_m^2\,\alpha_{mi}\alpha_{mj} \\ B_\beta &= \beta_{11}\beta_{22} - \beta_{12}^2 + \beta_{11}\beta_{33} - \beta_{13}^2 + \beta_{22}\beta_{33} - \beta_{23}^2.\end{aligned} \tag{16}$$

The turbulent viscosity is small in near-wall and transitional regions. The model seems to be promising for primary atomization where strong shear at the phase interface occurs. The constant $C_V = 2.5C_S^2$ is related to the Smagorinsky constant. The Kobayashi (K-C) (Kobayashi, 2005) or coherent structure model is based on the coherent structure function F_{CS} which is the second invariant Q of the velocity gradient tensor normalized by the magnitude E of the velocity gradient tensor. The coherent structure functions allows an appropriate damping near walls without the need of a damping function.

$$\begin{aligned}\nu_t^{K-C} &= C_K\,|F_{CS}|^{3/2}\,(1-F_{CS})\,\left|\overline{S}_{ij}\right| \\ F_{CS} &= \frac{Q}{E},\ Q = \frac{1}{2}\left(\overline{W}_{ij}\overline{W}_{ij} - \overline{S}_{ij}\overline{S}_{ij}\right),\ E = \frac{1}{2}\left(\overline{W}_{ij}\overline{W}_{ij} + \overline{S}_{ij}\overline{S}_{ij}\right)\end{aligned} \tag{17}$$

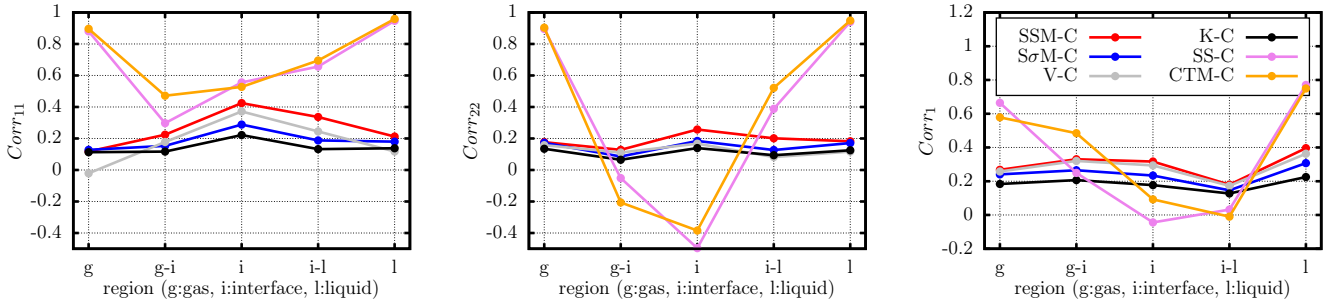

(a) (b) (c)

Figure 1: Correlation coefficients between the different closure models and the single subgrid stress components $\tau_{uu,ij}$ in axial and lateral jet direction (a-b) and the divergence of the subgrid stress $\frac{\partial}{\partial x_i}\tau_{uu,ij}$ in axial direction (c) evaluated in the gas and liquid flow 'g' and 'l', the area adjacent to the interface 'g-i' and 'i-l' and at the interface 'i'.

$$\bar{S}_{ij} = \frac{1}{2}\left(\frac{\partial \bar{u}_i}{\partial x_j} + \frac{\partial \bar{u}_j}{\partial x_i}\right),\ \bar{W}_{ij} = \frac{1}{2}\left(\frac{\partial \bar{u}_i}{\partial x_j} - \frac{\partial \bar{u}_j}{\partial x_i}\right)$$

The Kobayashi constant C_K is set to $C_K = 1/22$.

Besides eddy viscosity type models, also structural models can be used to close the convective subgrid term. The scale similarity model for the convective term, denoted as SS-C, reads

$$\frac{\partial}{\partial x_j}\tau^{SS-C}_{uu,ij} = \bar{\rho}\frac{\partial}{\partial x_j}\left(\widehat{\bar{u}_i\bar{u}_j} - \hat{\bar{u}}_i\hat{\bar{u}}_j\right) \tag{18}$$

where an additional secondary filter operation $\hat{\cdot}$ is involved. Clark's tensor diffusivity model CTM-C is based on a Taylor expansion for the filtered velocities which results in the following model expression

$$\frac{\partial}{\partial x_j}\tau^{CTM-C}_{uu,ij} = \bar{\rho}\frac{\partial}{\partial x_j}\left(\frac{\Delta^2}{12}\frac{\partial \bar{u}_i}{\partial x_k}\frac{\partial \bar{u}_j}{\partial x_k}\right). \tag{19}$$

Clark's model is based on first-order derivatives and does not involve explicit filter operations. Note that for both structural models the density is neither included in the filter operation nor in the gradient of the SGS stress term. This simplification is only valid in the two bulk phases. The density jump across the interface influences the models. The effect will be further investigated in future studies. None of the presented models for the SGS stress tensor needs to solve an additional transport equation.

The tensor $\tau_{nn,i}$ originates from subgrid interfacial deformation and includes the unresolved surface tension force to the momentum equation. The subgrid capillary force is modeled using the scale similarity hypothesis:

$$\tau^{SS-S}_{nn,i} = C_{nn}\cdot\sigma\left(\widehat{\bar{n}_i\bar{\kappa}\bar{\delta}_S} - \hat{\bar{n}}_i\hat{\bar{\kappa}}\hat{\bar{\delta}}_S\right) \tag{20}$$

The interfacial term $\tau_{\alpha u,i}$ is the subgrid term related to the interface transport which represents the interaction between the velocity and the interface. This correlation exists because the interface makes the velocity field anisotropic (Toutant et al., 2009) and has the characteristic of a turbulent scalar flux. The tensor affects the transport equation of the volume fraction Eq. (7) and makes approximately 10% of the advection term (Chesnel et al., 2011*a*) in primary atomization setups. A variety of models exists to close the term and a scale similarity type model

$$\tau^{SS-I}_{\alpha u,i} = C_{\alpha u}\cdot\left(\widehat{\bar{\alpha}\bar{u}_i} - \hat{\bar{\alpha}}\hat{\bar{u}}_i\right) \tag{21}$$

has been chosen. The secondary filtering $\hat{\cdot}$ is conducted with a filter proposed by Anderson and Domaradzki (2012). It has been shown that the order of magnitude of the diffusive subgrid term is negligible (Toutant et al., 2008; Vincent et al., 2008; Liovic and Lakehal, 2007; Ketterl and Klein, 2017) and therefore modeling is omitted within this work. The temporal term τ_{tt} will be included in future studies.

A-PRIORI ASSESSMENT

The round liquid jet is characterized by a Reynolds number based on the inlet velocity u_0 of $Re = 5000$ and a Weber number of $We = 2000$. The density and viscosity ratio of liquid to gas are set to $\rho_l/\rho_g = \mu_l/\mu_g = 40$ imitating a Diesel injection. A rectangular box of dimensions $12D \times 5D \times 5D$ where D denotes the jet diameter in the injection nozzle sets up the computational domain. The reference DNS is resolved with 128 equidistant control volumes across the nozzle diameter which corresponds to ≈ 630 Mio cells and a critical Weber number $We_{cr} = \rho_g u_0^2 \Delta x/\sigma = 15.625$.

A turbulent boundary condition is applied for the inflowing liquid stream in the injection nozzle. Turbulent velocity profiles with an integral length scale of $1/8D$ and a uniform fluctuation level of 7.5% superimposed to a mean hyperbolic-tangent profile in axial direction are generated by Klein's digital filter method (Klein et al., 2003). A modified Neumann condition which clips negative velocities is used at the outflow and slip is allowed at the side walls. In order to avoid the accumulation of droplets at the walls, the volume fraction is set to zero.

A-priori analysis allows to assess subgrid closures with respect to explicitly filtered DNS data. A Gaussian filter kernel which consists of the convolution of three one dimensional filters of the form $G(x) = \left(6/(\pi\Delta^2)\right)^{1/2}\exp(-6x^2/\Delta^2)$ with a filter size $\Delta = 4\Delta_{DNS}$ is applied to the DNS field to obtain the relevant reference data. The filtered field corresponds to an LES with 1/64 of the total DNS mesh resolution. Based on the filtered DNS quantities, a-priori investigations enable to evaluate the "exact" subgrid tensors (8)-(12). Further details are given in (Ketterl and Klein, 2017). The model performance is first evaluated based on a correlation analysis. Good agreement of the model expression is achieved if the correlation coefficient approaches unity whereas minus one represents a perfect negative correlation. Figure 1 shows the correlation strength of the proposed models with the SGS stress tensor. The correlation coefficient is plotted in five regions. The two bulk flows, the vicinity

Table 1: Correlation coefficients of the scale similarity models (SS-S, SS-I) for the surface tension τ_{nn} and interfacial subgrid term $\tau_{\alpha u}$ relative to the total domain.

	x	y	z
$Corr(\tau_{nn,i}, \tau_{nn,i}^{SS-S})$	0.45	0.55	0.55
$Corr(\tau_{\alpha u,i}, \tau_{\alpha u,i}^{SS-I})$	0.82	0.83	0.83

of the interface, the region towards the interface from the gas side and the region approaching the interface from the liquid phase. The two structural models show very high correlations in the bulk flow with constant density. Across the discontinuous interface, the SS-C and CTM-C model reveal negative correlations due to the model simplification of not including the density gradients. In contrast, correlations of eddy viscosity models slightly increase towards the interface but are in general weak. The damping behavior towards the interface of the SσM-C and K-C model does not significantly increase the correlation strength.

The correlation coefficients of the interfacial and surface tension subgrid term are listed in Tab. 1. Only the interface area is considered. The scale similarity models correlate reasonable with a correlation strength of ≈ 0.5 for the surface tension term and approaching 0.85 for the interfacial term. To emphasis the effect of these terms, the model constants are both set to $C_{nn} = C_{\alpha u} = 4$ in a-posteriori LES.

A-POSTERIORI COMPUTATIONS - DNS & LES

Within this section, a-posteriori LES including the different SGS models are discussend and results are compared to DNS data. Consistent with the a-priori analysis, the resolution for the LES is decreased to 32 cells per diameter which gives in total $\approx$ 9,8 Mio cells which reduces the computational effort by a factor of 256. With $We_{cr} = \rho_g u_0^2 \Delta x/\sigma = 62.5$, the resolution is too coarse to fulfill the criteria of $We_{cr} = \rho_g u_0^2 \Delta x/\sigma = 10$ (Desjardins and Pitsch, 2010) for fully resolved two-phase flow.

Figure 2 shows the liquid surface of the jet during the disintegration computed as DNS on top and LES on bottom. Interface instabilities and turbulence are fully resolved by the DNS. After the injection the wrinkling of the interface is more pronounced in the DNS. Thinner and more ligaments extrude from the liquid core. Consequently, a large number of drops separate, amongst many of them are very small in size, which cannot be captured by the LES mesh. The LES is not able to depict small scale interface instabilities without SGS modeling. Only large turbulent eddies interact with the interface which leads to less and bigger in size ligament formation. Hence, only few and big drops arise.

Besides the visual comparison, LES computations are quantitatvely assessed by statistical results and compared to DNS data. The LES flow data is averaged over 30,000 time steps which corresponds to 15 flow through times based on the centerline velocity. Assuming that the data is temporally uncorrelated after one integral time scale, 235 independent samples are obtained. Due to the immense computational effort, the DNS flow statistics are averaged over seven flow through times with 110 independant samples.

Figure 3 shows the axial development of the jet half width based on the velocity. In Fig. 3a an underresolved DNS (UDNS) is compared to LES including the subgrid models for the convective term computed with the QUICK advection scheme. The influence of all SGS stress models is small in general. Only for the SSM-C model, the jet half width increases less and the jet remains more compact. The SSM-C is known to overestimate the turbulent viscosity in the shear layer which leads to a dampening of turbulence-interface interactions and suppresses the development of interface instabilities. Table 2 shows an a-posteriori evaluation of the turbulent viscosity induced by the eddy viscosity models. Around 10.1% of the totally induced turbulent viscosity in the whole domain of the SSM-C model is introduced at the interface. This is reduced to 6.2% with the V-C which includes a specific treatment of shear layers. The SσM-C dampens the turbulent viscosity towards the interface even more to only 5.5%. Smallest turbulent viscosity is achieved with the K-C where only 3.1% are induced. Around the interface, a band of low turbulent viscosity is present (not shown here). Hence, the models which are originally developed for wall flows are able to transfer the damping behavior to some extend to interfacial flows using the analogy between a wall and a phase interface (Fulgosi et al., 2003).

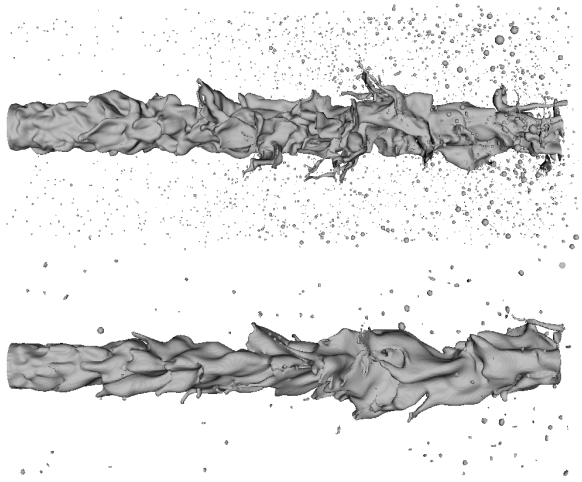

Figure 2: Liquid isosurface of a spatially developing round diesel jet computed as DNS (top) and LES (bottom).

The effect of including the subgrid surface tension force in the momentum equation and interfacial effects in the volume fraction equation is shown in Fig. 3b. The interfacial term has small influence on the jet half width. Incorporating subgrid surface tension forces however clearly enhances the jet breakup. The subgrid term increases the momentum exchange across the interface. Similar observations can be made in Fig. 4 which displays lateral plots of the standard deviation of the lateral velocity flucutation normalized with with centerline velocity U_{cl} and the jet half width $r_{1/2}$. Axial velocity velocity fluctuations $\sqrt{\langle u'u' \rangle}$ and cross correlations $\sqrt{\langle u'v' \rangle}$ show qualitatively similar behavior (not shown here). Not only the subgrid capillary forces but also the interfacial term promote the fluctuations in the shear layer.

The lateral profiles of the mean axial velocity scaled with the centerline velocity and the jet half width show the characteristic self similar behavior. The profiles do not differ independent of the advection scheme and subgrid model. The same holds true for volume concentration statistics. For the sake of brevity, results are not shown here.

Table 2: Percentage of the turbulent viscosity induced at the interface for different eddy viscosity models.

	SSM-C	SσM-C	V-C	K-C
$\nu_t(0 < \alpha < 1)/\nu_{t,total}$	10.1%	5.5%	6.2%	3.1%

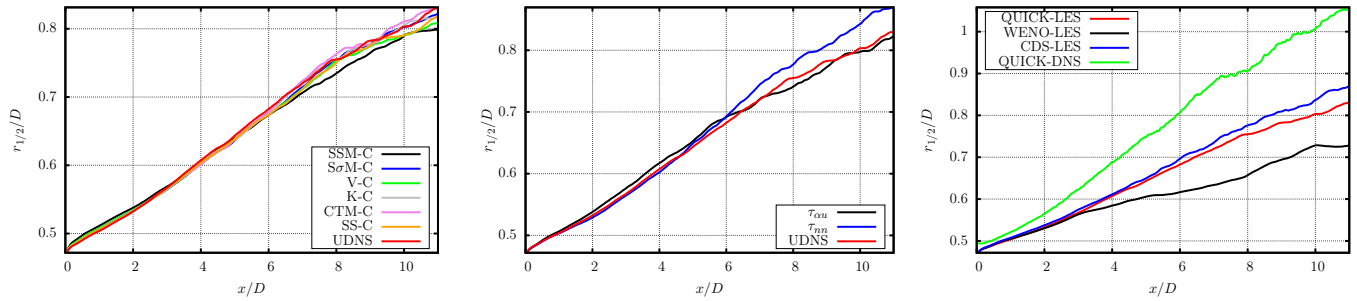

(a) (b) (c)

Figure 3: Axial development of the jet half width $r_{1/2}$ for the convective closure models (a) and surface tension and interfacial term (b) computed with the QUICK scheme and comparison of different advection discretization schemes (c).

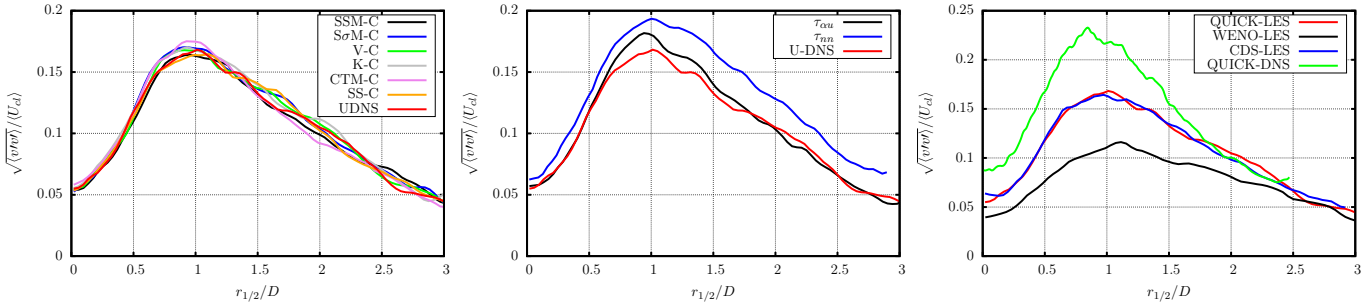

(a) (b) (c)

Figure 4: Lateral velocity fluctuations plotted against the lateral direction for the convective closure models (a) and surface tension and interfacial term (b) computed with the QUICK scheme and comparison of different advection discretization schemes (c) without the use of any subgrid models.

Figures 3c and 4c compare the jet half width and the lateral velocity fluctuations of the DNS with LES computed with different advection discretization schemes without the use of any subgrid model. Jet half width and fluctuations in the shear layer in the DNS result are significantly higher than for all LES simulations. Without appropriate SGS modeling, LES is not able to reproduce flow statistics of primary breakup obtained by a DNS resolving the full range of scales. A closer look to the different advection discretization schemes in the LES reveals that the difference of a second-order CDS and a third-order QUICK scheme is relatively small. It should be noted that the CDS produces unphyiscal oscillations if the flow is not fully resolved. Especially for higher Reynolds numebers, CDS is not a good choice since the reduced viscosity leads to very small time steps. These are necessary to allow diffusion to stabilise the computation. In contrast, if a WENO discretization scheme is used the jet remains clearly more compact and fluctuations are dampened in the shear layer. Compared with Figs. 4a and 3a, the influence of the applied advection discretization scheme to the flow statistics is larger than the influence of any of the SGS stress models. Consequently, it could be assumed that the numerical dissipation introduced by the advection scheme exceeds the influence of the SGS stress model. While assessing the numerical dissipation in a-posteriori computations is not straight forward, a-priori analysis allows an investigation of the error introduced by the advection discretization. Assuming that the CDS discretization is the "exact" solution, the difference to other advection schemes allows a categorization of the advection error. Table 3 lists this difference evaluated in the L_2 norm. Additionally, it is a-priori possible to estimate the order of magnitude of the SGS subgrid stress term $\frac{\partial}{\partial x_j}\tau_{\rho uu,ij}$, also shown in Tab. 3. The advection error in the bulk flow is of the same order of magnitude or even slightly higher than the SGS stress tensor. At the interface, the SGS stress tensor is bigger than the advection error due to large density gradients over the discontinuity but still is at the same order of magnitude.

Table 3: A-priori comparison of the order of magnitude of the SGS stress tensor $\left\| \frac{\partial}{\partial x_j}\tau_{\rho uu,ij} \right\|_2$ with the error between different discretization schems and a second-order central difference for the nonlinear advection e.g. $\left\| \frac{\partial}{\partial x_j}\left(u_i u_j\right)\Big|_{WENO} - \frac{\partial}{\partial x_j}\left(u_i u_j\right)\Big|_{CDS} \right\|_2$.

region	interface		bulk flow	
direction	axial	lateral	axial	lateral
$\left\| \frac{\partial}{\partial x_j}\tau_{\rho uu,ij} \right\|_2$	1944.8	1379.1	393.6	379.4
QUICK	796.3	664.5	472.2	422.2
WENO	974.6	973.7	665.4	703.9
TVD - Superbee	991.2	1041.7	751.6	807.4

The droplet size distribution is shown in Fig. 5. The distributions are averaged over independant 25 samples. The influence of eddy viscosity models relative to the underresolved DNS is small and exemplarily shown for the SσM-C model. With the SSM-C less droplets emerge due to the increased damping (not included in Fig. 5). The $\tau_{\alpha u,i}^{SS-I}$ model in the volume fraction equation has significant influence on the ligament dynamics. The coherent thin structures breakup later. Less and bigger droplets arise.

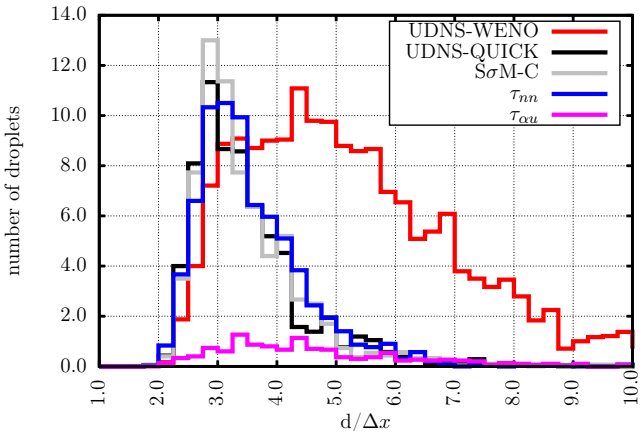

Figure 5: Averaged droplet size distribution obtained with different SGS models and different discretization schems for the advective term.

The droplet size distribution computed with the $\tau_{nn,i}^{SS-S}$ model expands and a plateau around the maximum appears. Altogether more drops separate when including subgrid surface tension forces. Similar to the conclusion for flow statistics, the advection scheme has the strongest influence on the droplet size. With WENO advection scheme, more and significantly bigger drops separate.

CONCLUSION

A-priori assessed subgrid models for two-phase LES have been evaluated in a-posteriori LES of primary breakup and and results are compared to DNS data. The influence of eddy viscosity models is in general low. The Smagorinsky models tends to suppress interface instabilities while the Kobayashi shows strongest damping behavior of turbulent viscosity towards the interface. Including SGS surface tension forces enhances the jet breakup and the SGS interfacial term reduces formation of small drops. It is shown that the influence of the numerical advection scheme is high and should be further investigated. Additionally, future subgrid model development should aim for an amplification of interface instabilities and promote jet breakup and be investigated for primary atomization at increased Reynolds and Weber numbers.

ACKNOWLEDGEMENT

Support by the German Research Foundation (Deutsche Forschungsgemeinschaft - DFG, GS: KL1456/1-1) is gratefully acknowledged. Computer resources for this project have been provided by the Gauss Centre for Supercomputing/Leibniz Supercomputing Centre under grant: pr48no. The authors also express their gratitude to the developers of the PARIS solver for providing the source code.

REFERENCES

Anderson, B. W. & Domaradzki, J. A. 2012 A subgrid scale model for large-eddy simulation based on the physics of interscale energy transfer in turbulence. *Physics of Fluids* **24** (6), 065104.

Arrufat, T., Dabiri, S., Fuster, D., Ling, Y., Malan, M., Scardovelli, R., Tryggvason, G., Yecko, P. & Zaleski, S. 2017 The paris-simulator code. *Available from http://www.ida.upmc.fr/ zaleski/paris* .

Chesnel, J., Menard, T., Reveillon, J. & Demoulin, F.-X. 2011*a* Subgrid analysis of liquid jet atomization. *Atomization and Sprays* **21** (1).

Chesnel, J., Reveillon, J., Menard, T. & Demoulin, F.-X. 2011*b* Large-eddy simulation of liquid jet atomization. *Atomization and Sprays* **21** (9).

De Villiers, E., Gosman, A. & Weller, H. 2004 Large-eddy simulation of primary diesel spray atomization. *Tech. Rep.*. SAE Technical Paper.

Desjardins, O. & Pitsch, H. 2010 Detailed numerical investigation of turbulent atomization of liquid jets. *Atomization and Sprays* **20** (4).

Fulgosi, M., Lakehal, D., Banerjee, S. & De Angelis, V. 2003 Direct numerical simulation of turbulence in a sheared air–water flow with a deformable interface. *Journal of Fluid Mechanics* **482**, 319–345.

Herrmann, M. 2013 A subgrid surface dynamics model for subfilter surface tension induced interface dynamics. *Computers & Fluids* **87**, 92–101.

Ketterl, S. & Klein, M. 2017 A-priori assessment of subgrid scale models for large-eddy simulation of liquid jet atomization. *submitted to International Journal of Multiphase Flow* .

Klein, M., Sadiki, A. & Janicka, J. 2003 A digital filter based generation of inflow data for spatially developing direct numerical or large-eddy simulations. *Journal of Computational Physics* **186** (2), 652–665.

Kobayashi, H. 2005 The subgrid-scale models based on coherent structures for rotating homogeneous turbulence and turbulent channel flow. *Physics of Fluids* **17** (4), 045104.

Labourasse, E., Lacanette, D., Toutant, A., Lubin, P., Vincent, S., Lebaigue, O., Caltagirone, J.-P. & Sagaut, P. 2007 Towards large eddy simulation of isothermal two-phase flows: governing equations and a-priori tests. *International Journal of Multiphase Flow* **33** (1), 1–39.

Liovic, P. & Lakehal, D. 2007 Multi-physics treatment in the vicinity of arbitrarily deformable gas–liquid interfaces. *Journal of Computational Physics* **222** (2), 504–535.

Nicoud, F., Toda, H. B., Cabrit, O., Bose, S. & Lee, J. 2011 Using singular values to build a subgrid scale model for large-eddy simulations. *Physics of Fluids (1994-present)* **23** (8), 085106.

Toutant, A., Chandesris, M., Jamet, D. & Lebaigue, O. 2009 Jump conditions for filtered quantities at an under-resolved discontinuous interface. part 1: Theoretical development. *International Journal of Multiphase Flow* **35** (12), 1100–1118.

Toutant, A., Labourasse, E., Lebaigue, O. & Simonin, O. 2008 Dns of the interaction between a deformable buoyant bubble and a spatially decaying turbulence: a-priori tests for LES two-phase flow modelling. *Computers & Fluids* **37** (7), 877–886.

Tryggvason, G., Dabiri, S., Aboulhasanzadeh, B. & Lu, J. 2013 Multiscale considerations in direct numerical simulations of multiphase flows. *Physics of Fluids (1994-present)* **25** (3), 031302.

Tryggvason, G., Scardovelli, R. & Zaleski, S. 2011 *Direct numerical simulations of gas–liquid multiphase flows*. Cambridge University Press.

Vincent, S., Larocque, J., Lacanette, D., Toutant, A., Lubin, P. & Sagaut, P. 2008 Numerical simulation of phase separation and a-priori two-phase LES filtering. *Computers & Fluids* **37** (7), 898–906.

Vreman, A. 2004 An eddy-viscosity subgrid-scale model for turbulent shear flow: Algebraic theory and applications. *Physics of fluids* **16** (10), 3670–3681.